CAN BLACK HOLE NEUTRINO-COOLED DISKS POWER SHORT GAMMA-RAY BURSTS?

Tong Liu[1,2,3,4], Yi-Qing Lin[5], Shu-Jin Hou[2,6], and Wei-Min Gu[1,4]
[1] Department of Astronomy and Institute of Theoretical Physics and Astrophysics, Xiamen University, Xiamen, Fujian 361005, China; tongliu@xmu.edu.cn
[2] Key Laboratory for the Structure and Evolution of Celestial Objects, Chinese Academy of Sciences, Kunming, Yunnan 650011, China
[3] State Key Laboratory of Theoretical Physics, Institute of Theoretical Physics, Chinese Academy of Sciences, Beijing 100190, China
[4] SHAO-XMU Joint Center for Astrophysics, Xiamen University, Xiamen, Fujian 361005, China
[5] School of Opto-electronic and Communication Engineering, Xiamen University of Technology, Xiamen, Fujian 361024, China
[6] College of Physics and Electronic Engineering, Nanyang Normal University, Nanyang, Henan 473061, China

ABSTRACT

Stellar-mass black holes (BHs) surrounded by neutrino-dominated accretion flows (NDAFs) are plausible sources of power for gamma-ray bursts (GRBs) via neutrino emission and their annihilation. The progenitors of short-duration GRBs (SGRBs) are generally considered to be compact binary mergers. According to the simulation results, the disk mass of the NDAF is limited after merger events. We can estimate such disk masses using the current SGRB observational data and fireball model. The results show that the disk mass of a certain SGRB mainly depends on its output energy, jet opening angle, and central BH characteristics. Even for the extreme BH parameters, some SGRBs require massive disks, which approach or exceed the limits in simulations. We suggest that there may exist alternative MHD processes or mechanisms that increase the neutrino emission to produce SGRBs with reasonable BH parameters and disk masses.

Key words: accretion, accretion disks – black hole physics – gamma-ray burst: general – neutrinos

1. INTRODUCTION

Gamma-ray bursts (GRBs) are the most powerful electromagnetic events in the universe; they are sorted into two categories, short- and long-duration GRBs (SGRBs and LGRBs; see Kouveliotou et al. 1993) or type I and II GRBs (Zhang 2006; Zhang et al. 2007a). Their progenitors are considered to be mergers of two compact objects, i.e., two neutron stars (NSs) or a black hole (BH) and an NS (for reviews see, e.g., Nakar 2007; Berger 2014), and collapses of massive stars (see, e.g., Woosley & Bloom 2006 for reviews), respectively. For interpreting the gamma-ray and afterglow emission of GRBs, the fireball shock model (for reviews, see, e.g., Mészáros 2002; Zhang & Mészáros 2004) has been widely accepted. The popular models for the central engines of GRBs are either a rotating stellar BH surrounded by a hyperaccretion disk (e.g., Paczyński 1991; Narayan et al. 1992; MacFadyen & Woosley 1999) or a quickly rotating magnetar (or protomagnetar, e.g., Usov 1992; Metzger et al. 2011; Lü et al. 2015).

Two mechanisms for powering GRBs have been proposed for when a hyperaccretion disk exists in a GRB's center: neutrino emission and annihilation, and MHD processes, such as the Blandford–Znajek (BZ) mechanism (Blandford & Znajek 1977) and episodic magnetic reconnection (Yuan & Zhang 2012). For the former mechanism, neutrino annihilation can produce a relativistic electron positron outflow, which is considered the progenitor of the fireball to power a GRB. The most probable model for launching a large number of neutrinos is a geometrically and optically thick neutrino-cooled hyper-accretion disk, referred to as a neutrino-dominated accretion flow (NDAF), whose typical characteristics are an extremely high accretion rate and a neutrino-cooling process. In the inner region of the NDAF, the main components are the electrons, free neutrons, and protons; the density and temperature are very high ($\rho \sim 10^{10} - 10^{13}$ g cm^{-3} and $T \sim 10^{10} - 10^{11}$ K), and the photons are tightly trapped in such disks, thus the energy loss is

mainly through neutrino and antineutrino radiation (see, e.g., Popham et al. 1999; Di Matteo et al. 2002; Kohri & Mineshige 2002; Rosswog & Ramirez-Ruiz 2002; Kohri et al. 2005; Lee et al. 2005; Gu et al. 2006; Chen & Beloborodov 2007; Kawanaka & Mineshige 2007; Liu et al. 2007; Zalamea & Beloborodov 2011; Janiuk et al. 2013; Kawanaka et al. 2013; Xue et al. 2013).

Two factors should be considered when calculating the neutrino luminosity and annihilation luminosity, which are the structure and components of the NDAF and the description of the relativistic neutrino propagation. Xue et al. (2013) investigated the global solutions of the radial structure and components of the NDAF in the Kerr spacetime of the BH with detailed neutrino physics and nucleosynthesis processes. The results show that the gas pressure and the neutrino cooling are always dominant in the inner region for the high-mass accretion rate, and the major components of the inner, middle, and outer regions are the free nucleons, ^{4}He, and ^{56}Fe, respectively. Importantly, they noticed that the radiative neutrinos mainly come from the inner region of the disk, and the neutrino emission rate depends less on the description of the microphysics (other studies of the NDAF model have also made this observation, e.g., Popham et al. 1999; Di Matteo et al. 2002; Liu et al. 2007; Kawanaka et al. 2013). Even for discussions of the vertical structure of the NDAF, similar solutions are presented (e.g., Liu et al. 2008, 2010, 2012a, 2013, 2014). Thus, the main problem is how to precisely calculate the neutrino annihilation processes. Birkl et al. (2007), Kovács et al. (2011a), and Kovács & Harko (2011b) analyzed the influence of general relativistic effects on the neutrino annihilation efficiency, which has a prominent increase compared with the Newtonian calculations. Based on the geodesic-tracing method, Zalamea & Beloborodov (2011) also studied annihilations via tracing the neutrino track.

For SGRBs, Eichler et al. (1989) proposed that the merger of two NSs might be candidates. Ruffert & Janka

(1998) simulated three-dimensional Newtonian hydrodynamical solutions of the merger events of two NSs with mass $\sim 1.6\, M_\odot$. There might survive a disk $\sim 0.1 - 0.2\, M_\odot$ surrounding a BH $\sim 2.5\, M_\odot$. Furthermore, Paczyński (1991) and Narayan et al. (1992) showed that the merger of an NS and a stellar-mass BH can also produce a SGRB. In simulations, the fragments of the NS can form a more massive disk, $\sim 0.5\, M_\odot$ (e.g., Kluźniak & Lee 1998; Lee & Kluźniak 1999; Popham et al. 1999; Liu et al. 2012b). In the past several years, the massive NSs, i.e., $\sim 2\, M_\odot$, have been discovered in binaries, which accompany white dwarfs (Demorest et al. 2010; Antoniadis et al. 2013). Yet we cannot neglect the possibility that massive NSs exist in BH–NS or two NSs binaries. However, the mass of the disk is still much smaller than $1\, M_\odot$ with a logical conjecture. This begs a question: can annihilations of neutrinos from NDAFs with such disk masses power all the observed SGRBs? Fan & Wei (2011) investigated the disk mass in the center of SGRBs with fixed values of the BH mass and spin. They found that nearly half of the SGRBs were suitable for the results of the above simulations. Here we consider the annihilation description, intact samples with prompt emission, afterglow properties of SGRBs, and reasonable ranges of the BH parameters as factors that should be fully addressed when answering the above question.

In Section 2, we describe the physical processes from the neutrino annihilation to observational gamma-ray photons. By using the current SGRB data, the disk masses for the definite ranges of the BH parameters are shown in Section 3. Conclusions and discussion are presented in Section 4.

2. MODEL

The neutrino annihilation luminosity $L_{\nu\bar{\nu}}$ is a function of the BH mass $M_{\rm BH}$, dimensionless spin parameter a_* ($a_* \equiv cJ/GM_{\rm BH}^2$, J is the angular momentum of the BH), dimensionless viscosity parameter α, and mass accretion rate $\dot{M}$ (see, e.g., Popham et al. 1999; Rosswog et al. 2003; Gu et al. 2006; Liu et al. 2007; Zalamea & Beloborodov 2011; Kawanaka et al. 2013; Xue et al. 2013; Leng & Giannios 2014).

The analytical formula for $L_{\nu\bar{\nu}}$ is shown in many previous works (e.g., Fryer et al. 1999; Zalamea & Beloborodov 2011; Xue et al. 2013). Here we adopt the neutrino annihilation luminosity $L_{\nu\bar{\nu}}$ given by Zalamea & Beloborodov (2011), which is expressed as

$$L_{\nu\bar{\nu}} \approx 5.7 \times 10^{52}\, x_{\rm ms}^{-4.8} \left(M_{\rm BH}/M_\odot\right)^{-3/2}$$
$$\times \begin{cases} 0 & \text{for } \dot{M} < \dot{M}_{\rm ign} \\ \left(\dot{M}/M_\odot\ {\rm s}^{-1}\right)^{9/4} & \text{for } \dot{M}_{\rm ign} < \dot{M} < \dot{M}_{\rm trap} \\ \left(\dot{M}_{\rm trap}/M_\odot\ {\rm s}^{-1}\right)^{9/4} & \text{for } \dot{M} > \dot{M}_{\rm trap} \end{cases}$$
$$\times\ {\rm erg\ s}^{-1}, \qquad (1)$$

where $x_{\rm ms} = r_{\rm ms}/r_g$, $r_{\rm ms}$ is the radius of the last (marginally stable) orbit, $r_g = 2GM_{\rm BH}/c^2$ is the Schwarzschild radius, $\dot{M}_{\rm ign}$ is the critical ignition accretion rate, and $\dot{M}_{\rm trap}$ is the accretion rate if neutrino trapping events occur in the inner region of the NDAF (e.g., Di Matteo et al. 2002; Kohri et al. 2005; Chen & Beloborodov 2007; Liu et al. 2012a; Xue et al. 2013). Their numerical results depend on the viscosity parameter α and BH

spin parameter a_*. Additionally, the value of viscosity parameter α has little effect on $L_{\nu\bar{\nu}}$ as long as $\dot{M}_{\rm ign} < \dot{M} < \dot{M}_{\rm trap}$ (Zalamea & Beloborodov 2011), so $\alpha = 0.1$ is adopted here. Furthermore, $x_{\rm ms}$ can be expressed as (e.g., Bardeen et al. 1972; Kato et al. 2008; Hou et al. 2014)

$$x_{\rm ms} = \frac{1}{2}\Big[3 + Z_2 - \sqrt{(3 - Z_1)(3 + Z_1 + 2Z_2)}\Big], \qquad (2)$$

where

$$Z_1 = 1 + \left(1 - a_*^2\right)^{1/3}\Big[\left(1 + a_*\right)^{1/3} + \left(1 - a_*\right)^{1/3}\Big], \qquad (3)$$

$$Z_2 = \sqrt{3a_*^2 + Z_1^2}. \qquad (4)$$

In comparison, Xue et al. (2013) also found a similar analytical solution, i.e., $L_{\nu\bar{\nu}} \propto \dot{M}^{2.17}$, but the influence of the BH mass was not considered.

Popham et al. (1999) and Liu et al. (2007) investigated the spatial distribution of the neutrino annihilation rate and found that nearly 60% of the total annihilation luminosity is ejected from the region $r < 20\, r_g$. In studies on the vertical structure of the NDAF model (e.g., Liu et al. 2010, 2012a, 2013), we found that the half-opening angle of the disk is very large, $\gtrsim 80°$, for the typical accretion rate, $\sim 1\, M_\odot\ {\rm s}^{-1}$, thus the empty funnel along the rotation axis above the disk can naturally limit the opening angle of the neutrino annihilable ejection to produce the primary fireball.

The fireball mean power outputting from the central engine $\dot{E}$ is a fraction of $L_{\nu\bar{\nu}}$, i.e.,

$$\dot{E} = \eta L_{\nu\bar{\nu}}, \qquad (5)$$

where η is the conversion factor (e.g., Aloy et al. 2005; Fan & Wei 2011; Liu et al. 2012b). The output power can be written as

$$\dot{E} \approx \frac{(1 + z)\left(E_{\gamma,\rm iso} + E_{k,\rm iso}\right)\theta_j^2}{2T_{90}}, \qquad (6)$$

where z is the redshift, $E_{\gamma,\rm iso}$ is the isotropic radiated energy in the prompt emission phase, $E_{k,\rm iso}$ is the isotropic kinetic energy of the outflow powering long-lasting afterglow, T_{90} can roughly be considered the duration of the activity of the central engine, and θ_j is the opening angle of the ejecta.

Hence, for the cases $\dot{M}_{\rm ign} < \dot{M} < \dot{M}_{\rm trap}$, we have the mean accretion rate (Fan & Wei 2011)

$$\dot{M} \approx 0.12 \left[\frac{(1 + z)\left(E_{\gamma,\rm iso,51} + E_{k,\rm iso,51}\right)\theta_j^2}{\eta T_{90,s}}\right]^{4/9}$$
$$\times\ x_{\rm ms}^{2.1} \left(\frac{M_{\rm BH}}{M_\odot}\right)^{2/3} M_\odot\ {\rm s}^{-1}, \qquad (7)$$

where $E_{k,\rm iso,51} = E_{k,\rm iso}/(10^{51}\ {\rm ergs})$, $E_{\gamma,\rm iso,51} = E_{\gamma,\rm iso}/(10^{51}\ {\rm ergs})$, and $T_{90,s} = T_{90}/(1\ {\rm s})$.

Furthermore, the disk mass is

$$M_{\text{disk}} \approx 0.12 \left[\frac{\left(E_{\gamma,\text{iso},51} + E_{k,\text{iso},51} \right) \theta_j^2}{\eta} \right]^{4/9}$$

$$\left(\frac{T_{90,s}}{1+z} \right)^{5/9} x_{\text{ms}}^{2.1} \left(\frac{M_{\text{BH}}}{M_\odot} \right)^{2/3} M_\odot. \tag{8}$$

According to Equation (8), we can estimate the disk mass by using the observational data. It should be noted that there exist some uncertainties, especially for the efficiency η and the interval of the activity of the central engine replaced by T_{90}. There should exist an efficiency from the neutrino annihilation to the initial fireball, then to the jet kinetic energy and radiation, which is mainly related to the energy, components, and state of the fireball (e.g., Eichler et al. 1989; Aloy et al. 2005). Aloy et al. (2005) mentioned that the duration of the GRB event might be longer than the time interval of the activity of the central engine if the radial expansion of the fireball is considered. In the fireball model, it is difficult to estimate the duration of such an expansion to the optically thin phase using the observational data unless the blackbody component can be observed. It is conceivable that the consequences of the use of η and T_{90} would change the resulting disk mass to some extent, although the exponents of η and T_{90} in Equation (8) are small.

$E_{\gamma,\text{iso}}$ can be calculated by the observational data, which is written as

$$E_{\gamma,\text{iso}} = 4\pi D_L^2 F_\gamma / (1+z), \tag{9}$$

where D_L is the luminosity distance and F_γ is the fluence in the 15–150 keV for *Swift* events. Then D_L is defined as

$$D_L = \frac{(1+z)c}{H_0} \int_0^z \left[\Omega_M (1+z')^3 + \Omega_\Lambda \right]^{-1/2} dz', \tag{10}$$

where we employ a standard ΛCDM cosmology model with $\Omega_M = 0.27$, $\Omega_\Lambda = 0.73$, and $H_0 = 71$ km s^{-1} Mpc^{-1}. Moreover, the mean isotropic gamma-ray luminosity is

$$L_{\gamma,\text{iso}} \approx E_{\gamma,\text{iso}} (1+z) / T_{90}. \tag{11}$$

$E_{k,\text{iso}}$ and θ_j can be deduced from the modeling of the X-ray afterglow data. We take $E_{k,\text{iso}}$ as (Lloyd-Ronning & Zhang 2004; Fan & Piran 2006; Zhang et al. 2007b)

$$E_{k,\text{iso}} \approx 9.2 \times 10^{52} R L_{X,46}^{4/(p+2)} \left(\frac{1+z}{2} \right)^{-1}$$

$$\times \epsilon_{B,-2}^{(2-p)/(p+2)} \epsilon_{e,-1}^{4(1-p)/(p+2)}$$

$$\times t_d^{(3p-2)/(p+2)} (1+Y)^{4/(p+2)} \text{ ergs}, \tag{12}$$

where $R \sim (t_{11}/T_{90,s})^{17\epsilon_e/16}$ is a factor that accounts for the energy loss during the deceleration following the prompt gamma-ray emission phase (e.g., Sari 1997; Lloyd-Ronning & Zhang 2004), $\epsilon_{e,-1} = \epsilon_e / 0.1$ is the fraction of shock energy given to the electrons, $\epsilon_{B,-2} = \epsilon_B / 0.01$ is the fraction of energy in the magnetic field, $t_{11} = t/(11 \text{ hr})$ and $t_d = t/(1 \text{ day})$ are the times of observation, Y is the Compton parameter, p is the energy distribution index of the shock-accelerated electrons and can be fitted by the observed photon index in the X-ray spectrum (e.g., Zhang et al. 2006; Gao et al. 2013), and

$L_{X,46} = L_X / (10^{46} \text{ erg s}^{-1})$ is the isotropic X-ray afterglow luminosity. Here we take the X-ray luminosity at 11 hr since the burst triggers, which can be written as

$$L_X = 4\pi D_L^2 F_X, \tag{13}$$

where F_X is the X-ray flux of the afterglow recorded by satellites.

Furthermore, the relation between the opening angle and the jet break time is given by (e.g., Sari et al. 1999; Frail et al. 2001; Fong et al. 2012)

$$\theta_j \approx 0.076 \left(\frac{t_j}{1 \text{ day}} \right)^{3/8} \left(\frac{1+z}{2} \right)^{-3/8}$$

$$\times \left(\frac{n}{0.01 \text{ cm}^{-3}} \right)^{1/8} E_{k,\text{iso},51}^{-1/8}, \tag{14}$$

where t_j is the jet break time in the X-ray afterglow phase of GRBs, and n is the number density of the burst circumstance.

3. RESULTS

The relations among the observational data of the prompt emission and afterglow in SGRBs, disk mass, and BH parameters are established by Equations (8)–(14). If reasonable ranges of the BH parameters are given, the limits of the disk masses corresponding to certain SGRBs can be resolved.

3.1. Data of SGRBs

Berger (2014) mainly reviewed the progress of SGRBs in theories and observations, including the afterglow and host galaxy observations, the properties of the circumburst environments, and their progenitors. There are 70 SGRBs with a substantial fraction of afterglow detections in the eight-year period from 2005 January to 2013 January (Berger 2014), with the addition of GRB 130603B (e.g., Berger et al. 2013; Tanvir et al. 2013), which is associated with a kilonova (Li & Paczyński 1998). As shown in Table 1 of Berger (2014), there are 27 SGRBs with authentic X-ray detections and known redshifts discovered by *Swift*, except for GRB 050709 by *HETE*-2.

Moreover, we find four SGRBs with X-ray detections and known redshifts triggered after GRB 130603B, i.e., GRBs 131001A, 140622A, 140903A, and 141212A, whose data are from the UK Swift Science Data Centre (Evans et al. 2009). So in total, 31 SGRBs are listed in Table 1. For each SGRB, we fit the photon index with the data of the X-ray spectrum to deduce p (e.g., Zhang et al. 2006; Gao et al. 2013). Their durations T_{90}, redshifts z, gamma-ray fluences F_γ and X-ray fluxes at 11 hr since trigger F_X (11 hr), and the observed spectral index β are displayed. If we take $\epsilon_e \sim 0.1$, $\epsilon_B \sim 0.01$, $Y \sim 0$, $\eta = 0.3$, and the fitted p and given t_j, then $E_{\gamma,\text{iso}}$, $E_{k,\text{iso}}$, and θ_j can be solved, and we further obtain the ranges of the disk masses.

It is worth noting that the most difficult problem is the estimation of the jet opening angle θ_j because of the faint and restricted observations of SGRB afterglows. So far there are three scenarios: (1) a few credible detections of a jet break, such as in GRBs 051221A (Soderberg et al. 2006), 090426 (Nicuesa Guelbenzu et al. 2011), and 130603B (Fong & Berger 2013); (2) several meaningful lower limits on jet opening angles, such as in GRBs 050724 (Grupe et al. 2006), 111117A (Margutti et al. 2012), and 120804A (Berger

Table 1
Data of SGRBs

GRB	T_{90} (s)	z	F_γ (10^{-7} erg cm^{-2})	F_X(11 hr) (10^{-14} erg cm^{-2} s^{-1})	Photon Index	$E_{\gamma,\mathrm{iso}}$ (10^{51} ergs)	$E_{k,\mathrm{iso}}$[a] (10^{51} ergs)	θ_j (rad)	M_{disk}[b] ($M_\odot$)
050509B	0.04	0.225	0.23	<1.95	$1.6^{+0.5}_{-0.4}$	0.0027	0.055	$\gtrsim 0.05$	0.0006–0.028
050709	0.07	0.161	4.0	1.92	~ 2	0.023	0.016	$\gtrsim 0.26$ (1)	0.003–0.14
050724	3	0.257	6.3	9.55	$1.68^{+0.15}_{-0.13}$	0.1	0.27	$\gtrsim 0.35$ (2)	0.084–3.93
051210	1.3	1.3	0.83	<2.7	$2.78^{+0.48}_{-0.41}$	0.36	2.38	$\gtrsim 0.05$	0.016–0.76
051221A	1.4	0.5465	12	108	$2.09^{+0.10}_{-0.09}$	0.92	12.6	~ 0.12 (3)	0.093–4.37
060502B	0.09	0.287	0.4	<1.47	$2.15^{+1.07}_{-0.58}$	0.012	0.12	$\gtrsim 0.05$	0.0013–0.062
060801	0.5	1.130	0.81	<0.98	$2.01^{+0.23}_{-0.26}$	0.27	0.71	$\gtrsim 0.05$	0.0063–0.30
061006	0.4	0.438	14	22.7	$1.86^{+0.30}_{-0.24}$	0.67	3.14	$\gtrsim 0.05$	0.013–0.59
061201	0.8	0.111	3.3	19.2	$1.54^{+0.17}_{-0.17}$	0.01	0.07	~ 0.017 (4)	0.0014–0.067
061210	0.2	0.409	3.0	13.6	$2.60^{+1.92}_{-0.71}$	0.12	0.86	$\gtrsim 0.05$	0.0048–0.22
070429B	0.5	0.902	0.63	11.3	$2.69^{+1.18}_{-0.56}$	0.13	4.51	$\gtrsim 0.05$	0.013–0.63
070714B	2.0	0.923	7.2	6.30	$1.96^{+0.12}_{-0.15}$	1.61	2.32	$\gtrsim 0.05$	0.027–1.25
070724A	0.4	0.457	0.30	12.8	$1.46^{+0.36}_{-0.25}$	0.016	0.99	$\gtrsim 0.05$	0.007–0.33
070729	0.9	0.8	1.0	<4.71	$1.5^{+0.6}_{-0.3}$	0.17	1.32	$\gtrsim 0.05$	0.012–0.54
070809	1.3	0.473	1.0	53.0	$1.39^{+0.14}_{-0.12}$	0.056	3.91	$\gtrsim 0.05$	0.024–1.15
071227	1.8	0.381	2.2	3.20	$2.19^{+0.41}_{-0.35}$	0.08	0.25	$\gtrsim 0.05$	0.01–0.47
080905A	1.0	0.122	1.4	<6.7	$1.54^{+0.22}_{-0.14}$	0.005	0.024	$\gtrsim 0.05$	0.0027–0.13
090426	1.2	2.609	1.8	26.3	$2.03^{+0.16}_{-0.15}$	2.84	135	~ 0.07 (5)	0.093–4.35
090510	0.3	0.903	3.4	5.04	$1.70^{+0.12}_{-0.12}$	0.73	3.07	~ 0.017 (4)	0.0035–0.17
090515	0.04	0.403	0.21	<8.43	$2.73^{+1.20}_{-0.77}$	0.008	0.62	$\gtrsim 0.05$	0.0016–0.075
100117A	0.3	0.915	0.93	<2.50	$2.74^{+0.36}_{-0.31}$	0.20	1.10	$\gtrsim 0.05$	0.0057–0.27
100206A	0.1	0.408	1.4	<1.07	$2.0^{+0.8}_{-0.7}$	0.058	0.073	$\gtrsim 0.05$	0.0013–0.062
100625A	0.3	0.453	2.3	0.395	$2.3^{+0.5}_{-0.3}$	0.12	0.093	$\gtrsim 0.05$	0.003–0.14
101219A	0.6	0.718	4.6	2.00	$1.44^{+0.27}_{-0.25}$	0.62	0.45	$\gtrsim 0.05$	0.008–0.38
111117A	0.5	1.3	1.4	3.21	$2.10^{+0.39}_{-0.32}$	0.62	3.77	0.105 (6)	0.023–1.06
120804A	0.81	1.3	8.8	58.6	$2.10^{+0.22}_{-0.14}$	3.88	56.9	$\gtrsim 0.19$ (7)	0.16–7.59
130603B	0.18	0.356	6.3	60.0	$2.00^{+0.14}_{-0.13}$	0.20	2.80	~ 0.07 (8)	0.01–0.48
131001A	1.54	0.717	2.8	14.7	$1.91^{+0.18}_{-0.18}$	0.37	5.41	$\gtrsim 0.05$	0.029–1.37
140622A	0.13	0.959	0.27	17.0	$1.55^{+0.67}_{-0.28}$	0.065	9.77	$\gtrsim 0.05$	0.0087–0.41
140903A	0.30	0.351	1.4	124.7	$1.59^{+0.22}_{-0.20}$	0.043	6.15	0.023 (9)	0.0067–0.31
141212A	0.30	0.596	0.72	2.50	$2.0^{+0.8}_{-0.5}$	0.066	0.38	$\gtrsim 0.05$	0.0039–0.18

Notes.
[a] The parameters are calculated using Equation (12) with $\epsilon_e \sim 0.1$, $\epsilon_B \sim 0.01$, and $Y \sim 0$.
[b] The ranges of M_{disk} are estimated by Equation (8) with $\eta = 0.3$, varying M_{BH} from 2.7 $M_\odot$ to 10 $M_\odot$, and a_* from 0 to 0.99.

References. (1) Berger (2014), (2) Grupe et al. (2006), (3) Soderberg et al. (2006), (4) De Pasquale et al. (2010), Nicuesa Guelbenzu et al. (2012), (5) Nicuesa Guelbenzu et al. (2011), (6) Margutti et al. (2012), (7) Berger et al. (2013), (8) Fong & Berger (2013), (9) The opening angle of GRB 140903A is determined by Equation (14) with the data from the UK Swift Science Data Centre (Evans et al. 2009) and $n \sim 0.01$ cm^{-3}.

et al. 2013); and (3) no break in X-ray light curves of some SGRBs. We cite the data of the jet opening angles or their lower limits in the above references for the former two cases, as shown in Table 1. For the third scenario, we set a lower limit of $\theta_j \gtrsim 0.05$ (Fong et al. 2012). For the last four SGRBs we collected, the jet break time, $\sim 3.80^{+0.00}_{-2.50}$ ks, is found in GRB 140903, which allows us to estimate the opening angle using Equation (14) with $n = 0.01$ cm^{-3}, and the other three are set by the lower limit as discussed above.

3.2. Disk Masses of SGRBs

Figure 1 shows the ranges of disk masses M_{disk} of the different SGRBs with the isotropic gamma-ray luminosity $L_{\gamma,\mathrm{iso}}$ for varying BH mass M_{BH} from 2.7 $M_\odot$ to 10 $M_\odot$ and BH spin a_* from 0 to 0.99. Three vertical lines correspond to $M_{\mathrm{disk}} = 0.2\, M_\odot$, 0.5 $M_\odot$, and 1 $M_\odot$, respectively. It is seen that

M_{disk} has a wide distribution, from about $6 \times 10^{-4}\, M_\odot$ to about 7.6 $M_\odot$, as shown in Table 1. The accretion rates corresponding to the minimal disk masses are checked, which are in suitable ranges, i.e., $\dot{M}_{\mathrm{ign}} < \dot{M} < \dot{M}_{\mathrm{trap}}$. There is no statistical correlation between the disk mass and the gamma-ray isotropic luminosity because the energy coming from the accretion powers all of the radiative processes of GRBs, mainly in gamma-ray and X-ray bands. The energies of the X-ray afterglows are frequently larger than those of prompt emission as displayed in Table 1. The disk mass is primarily calculated by the output energy of GRBs, opening angle of the jet, and BH characteristics as shown in Equation (8). There exists a difference of several orders of magnitude between the minimal and maximal disk masses, which means that the BH characteristics are the major factors in the disk mass.

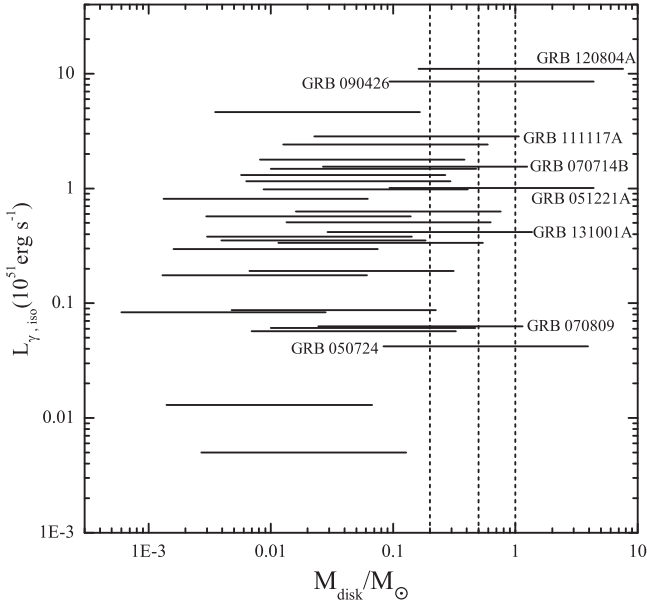As shown in the figure, the maximal disk masses of GRBs 050724, 051221A, 070714B, 070809, 090426, 111117A,

Figure 1. Ranges of disk masses M_{disk} of different SGRBs with isotropic gamma-ray luminosity $L_{\gamma,iso}$ for varying BH mass M_{BH} from 2.7 $M_\odot$ to 10 $M_\odot$ and BH spin a_* from 0 to 0.99. Three vertical lines correspond to $M_{disk} = 0.2\ M_\odot$, $0.5\ M_\odot$, and 1 $M_\odot$, respectively.

120804A, and 131001A are larger than 1 $M_\odot$, and that of most other SGRBs in our sample are larger than 0.2 $M_\odot$, which indicates that extreme BH spin parameters and small BH mass are required. In binary NS merger events, the BH mass is naturally less than the total mass of the binary, i.e., $\sim 4\ M_\odot$, which is described as about $\sim 2.7\ M_\odot$ in further simulations. In BH–NS binaries, the BH originates from its progenitor star, and its mass should also be a stellar-mass order, e.g., $\sim 10\ M_\odot$. Moreover, the BH spin parameters are also related to their progenitors. In some discussions (e.g., Lee et al. 2000b; Ruffert & Janka 2001) the rapidly rotating BHs ($a_* \geqslant 0.5$) are inclined to exist in the SGRB centers, in contrast to the BHs in the LGRB centers.

In order to embody the effects of the BH characteristics on the disk mass, we display in Figure 2 the distributions of the disk masses M_{disk} for the different typical BH masses and spins, which are set to $(M_{BH}/M_\odot, a_*) = (3, 0.5)$, $(3, 0.9)$, $(10, 0.5)$, and $(10, 0.9)$, corresponding to (a)–(d), respectively. It is clear that the disk masses of most SGRBs are safely below $0.2-0.4\ M_\odot$, and sporadic cases are beyond the limits, especially in the case of Figure 2(c). Additionally, by comparing these four cases, we notice that the spin parameters have more of an effect than the BH masses on the values of the disk masses. Even for the case of Figure 2(b), there still exists one SGRB whose disk mass is larger than 0.45 $M_\odot$. Those massive disks, $\geqslant 1\ M_\odot$, may exist in the centers of collapsars, which are considered the origin of LGRBs. Lazzati et al. (2010) have actually proposed that the off-axis jets from collapsars could power SGRBs.

Three factors remind us that the results of the disk masses are at most the lower limits. (1) We have to calculate the disk mass using the lower limit of θ_j in most SGRBs as shown in Table 1. It is easily conceivable that the real requirements for the disk masses are much larger than the present results if the precise value of θ_j is considered. (2) Some powerful SGRBs with unknown redshift, such as GRBs 060121, 060313, and

111121A, which are shown in Table 1 of Berger (2014), may require more massive disks than the SGRBs in our sample if they also originate from the BH hyperaccretion systems. (3) The powerful X-ray flares have been extensively observed in the afterglow phase of GRBs, which are considered to originate from the re-ignition of the central engine (e.g., Liu et al. 2008; Luo et al. 2013; Hou et al. 2014). This means that remnant matter from the massive disks is needed to maintain the explosion of X-ray flares. However, we use T_{90} to replace the duration of the activity of the central engine, which may generally enlarge the disk mass in the calculations. Although these influences and some uncertainties may exist, we contend that our results can still reflect the deficiency of the neutrino annihilation process to power SGRBs.

4. CONCLUSIONS AND DISCUSSION

Compact binary merger events are considered the progenitors of SGRBs. After a merger, a stellar-mass BH surrounded by an NDAF will be formed in the central SGRB and neutrino–antineutrino annihilation above the disk may power the SGRB. The total mass of two compact stars limits the mass of the system consisting of a BH and an NDAF. In this paper, we focus on this question: can annihilations of neutrinos from NDAFs owning such masses power all the observed SGRBs? The calculations show that the disk mass of a certain SGRB mainly depends on its output energy, jet opening angle, and central BH characteristics. Even for the extreme BH parameters, there still exist some SGRBs that require massive disks, which can approach or exceed the limits in simulations.

Besides the magnetar model, for BH hyperaccretion systems, we suggest that there may exist an alternative magnetic origin of SGRBs, i.e., the BZ process (e.g., Popham et al. 1999; Lee et al. 2000a, 2000b; Di Matteo et al. 2002; Kawanaka et al. 2013) or episodic magnetic reconnection (Yuan & Zhang 2012), for replacing neutrino annihilation. Kawanaka et al. (2013) found that luminosity powered by a Poynting-dominated jet is more qualified for the requirements of GRBs than neutrino pair annihilation. Yuan & Zhang (2012) investigated the closed magnetic field lines that continuously emerge out of the accretion flow. Since the motion of the accretion flow is shear and turbulent, the line may form the flux rope. When a threshold is reached, the system loses its equilibrium and the flux rope is thrust outward, and then an episodic jet occurs. This mechanism can provide the enormous amount of energy needed to trigger GRBs. In addition, if these magnetic origins really exist in the center of GRBs, the polarization effect should be observed in the prompt emission or afterglow of GRBs. In fact, linear polarization in the afterglow of LGRB GRB 120308 has been detected (Mundell et al. 2013), which indicates that large-scale magnetic fields may be dominant in GRB jets. But now we do not know whether the same situation exists in SGRBs.

Alternatively, there are some mechanisms, such as magnetic coupling from the BH horizon to the inner region of the disk (Li 2000), that can effectively transfer the angular momentum and rotational energy of the BH to heat the inner region of the disk, then radiate larger numbers of neutrinos from the disk to produce the primordial fireball (e.g., Lei et al. 2009; Luo et al. 2013). Additionally, the vertical advection (or convection) is considered to widely exist in the slim disks and the NDAFs (Jiang et al. 2014; Liu et al. 2015), which suggests another possible mechanism for increasing the neutrino
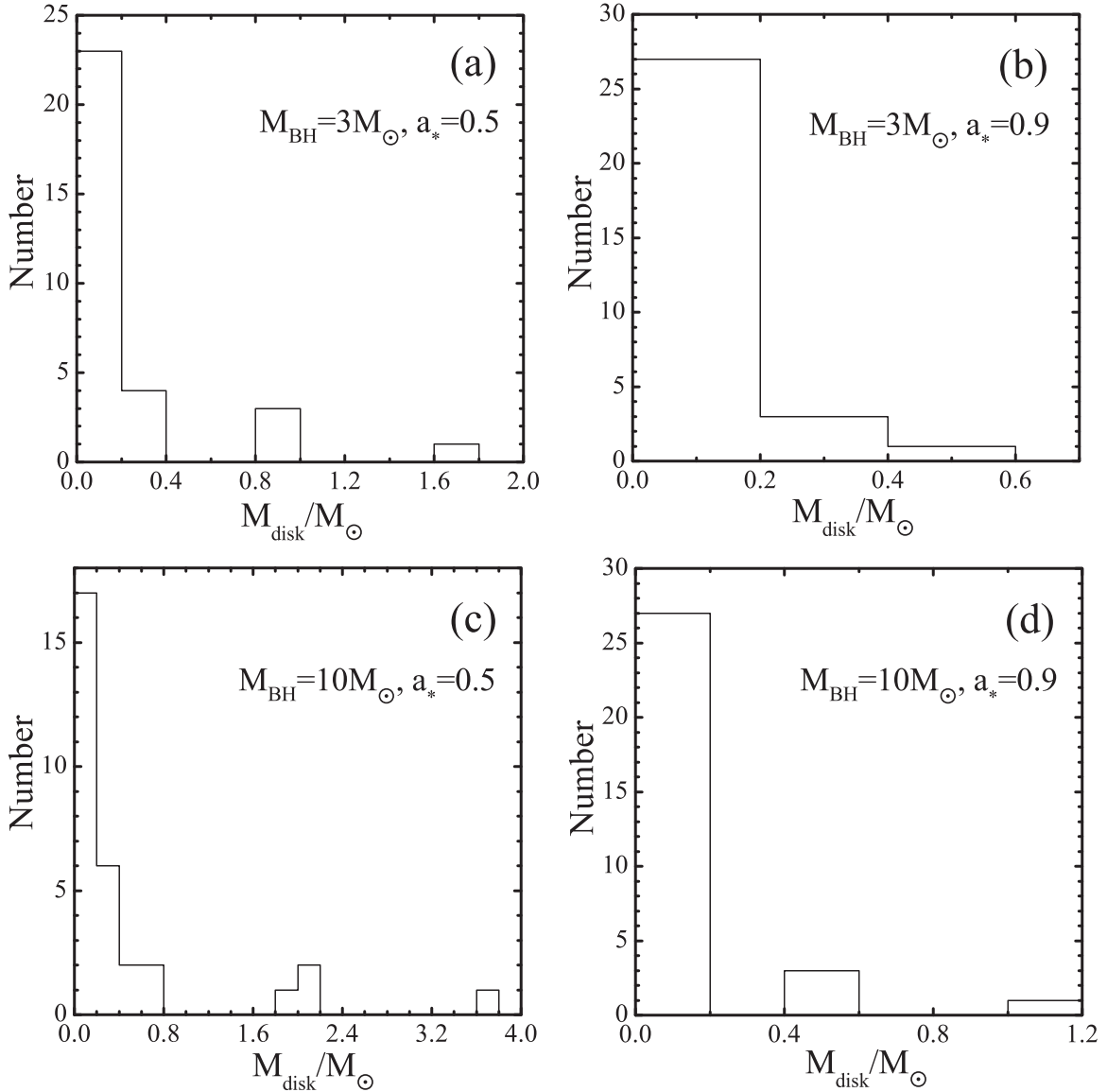
Figure 2. Distributions of the disk masses M_{disk} for different typical BH masses and spins.

emission rate. The scenario for NDAFs is as follows: the vertical advection (or convection) caused by magnetic buoyancy effectively transports energy to the disk surface and also suppresses the radial advection, thus the neutrino luminosity and annihilation luminosity are dramatically increased. This mechanism is conducive for achieving the energy requirement of GRBs.

REFERENCES

Aloy, M. A., Janka, H.-T., & Müller, E. 2005, A&A, 436, 273
Antoniadis, J., Freire, P. C. C., Wex, N., et al. 2013, Sci, 340, 448
Bardeen, J. M., Press, W. H., & Teukolsky, S. A. 1972, ApJ, 178, 347
Berger, E. 2014, ARA&A, 52, 43
Berger, E., Fong, W., Chornock, R., et al. 2013, ApJL, 774, L23
Birkl, R., Aloy, M. A., Janka, H.-T., & Müller, E. 2007, A&A, 463, 51
Blandford, R. D., & Znajek, R. L. 1977, MNRAS, 179, 433
Chen, W. X., & Beloborodov, A. M. 2007, ApJ, 657, 383
Demorest, P. B., Pennucci, T., Ransom, S. M., Roberts, M. S. E., & Hessels, J. W. T. 2010, Natur, 467, 1081
De Pasquale, M., Schady, P., Kuin, N. P. M., et al. 2010, ApJL, 709, L146
Di Matteo, T., Perna, R., Narayan, R., et al. 2002, ApJ, 579, 706
Eichler, D., Livio, M., Piran, T., & Schramm, D. N. 1989, Natur, 340, 126
Evans, P. A., Beardmore, A. P., Page, K. L., et al. 2009, MNRAS, 397, 1177
Fan, Y., & Piran, T. 2006, MNRAS, 369, 197
Fan, Y.-Z., & Wei, D.-M. 2011, ApJ, 739, 47
Fong, W., & Berger, E. 2013, ApJ, 776, 18
Fong, W., Berger, E., Margutti, R., et al. 2012, ApJ, 756, 189
Frail, D. A., Kulkarni, S. R., Sari, R., et al. 2001, ApJL, 562, L55

Fryer, C. L., Woosley, S. E., Herant, M., & Davies, M. B. 1999, ApJ, 520, 650
Gao, H., Lei, W.-H., Zou, Y.-C., Wu, X.-F., & Zhang, B. 2013, NewAR, 57, 141
Grupe, D., Burrows, D. N., Patel, S. K., et al. 2006, ApJ, 653, 462
Gu, W.-M., Liu, T., & Lu, J.-F. 2006, ApJL, 643, L87
Hou, S.-J., Liu, T., Gu, W.-M., et al. 2014, ApJL, 781, L19
Janiuk, A., Mioduszewski, P., & Moscibrodzka, M. 2013, ApJ, 776, 105
Jiang, Y.-F., Stone, J. M., Davis, S. W., et al. 2014, ApJ, 796, 106
Kato, S., Fukue, J., Mineshige, S., et al. 2008, Black-Hole Accretion Disks: Towards a New Paradigm (Kyoto: Kyoto Univ. Press)
Kawanaka, N., & Mineshige, S. 2007, ApJ, 662, 1156
Kawanaka, N., Piran, T., & Krolik, J. H. 2013, ApJ, 766, 31
Kohri, K., & Mineshige, S. 2002, ApJ, 577, 311
Kohri, K., Narayan, R., & Piran, T. 2005, ApJ, 629, 341
Kluźniak, W., & Lee, W. H. 1998, ApJL, 494, L53
Kouveliotou, C., Meegan, C. A., Fishman, G. J., et al. 1993, ApJL, 413, L101
Kovács, Z., Cheng, K. S., Harko, T., et al. 2011a, MNRAS, 411, 1503
Kovács, Z., & Harko, T. 2011b, MNRAS, 417, 2330
Lazzati, D., Morsony, B. J., & Begelman, M. C. 2010, ApJ, 717, 239
Lee, H. K., Brown, G. E., Wijers, R. A. M. J., et al. 2000a, ApJ, 536, 416
Lee, H. K., Wijers, R. A. M. J., Brown, G. E., et al. 2000b, PhR, 325, 83
Lee, W. H., & Kluźniak, W. 1999, ApJ, 526, 178
Lee, W. H., Ramirez-Ruiz, E., & Page, D. 2005, ApJ, 632, 421
Lei, H. H., Wang, D. X., Zhang, L., et al. 2009, ApJ, 700, 1970
Leng, M., & Giannios, D. 2014, MNRAS, 445, L1
Li, L.-X. 2000, ApJL, 533, L115
Li, L.-X., & Paczyński, B. 1998, ApJL, 507, L59
Liu, T., Gu, W.-M., Dai, Z.-G., & Lu, J.-F. 2010, ApJ, 709, 851
Liu, T., Gu, W.-M., Kawanaka, N., & Li, A. 2015, ApJ, 805, 37
Liu, T., Gu, W.-M., Xue, L., & Lu, J.-F. 2007, ApJ, 661, 1025
Liu, T., Gu, W.-M., Xue, L., Weng, S.-S., & Lu, J.-F. 2008, ApJ, 676, 545
Liu, T., Gu, W.-M., Xue, L., & Lu, J.-F. 2012a, Ap&SS, 337, 711
Liu, T., Liang, E.-W., Gu, W.-M., et al. 2012b, ApJ, 760, 63
Liu, T., Xue, L., Gu, W.-M., & Lu, J.-F. 2013, ApJ, 762, 102
Liu, T., Yu, X.-F., Gu, W.-M., & Lu, J.-F. 2014, ApJ, 791, 69
Lloyd-Ronning, N. M., & Zhang, B. 2004, ApJ, 613, 477
Luo, Y., Gu, W.-M., Liu, T., & Lu, J.-F. 2013, ApJ, 773, 142
Lü, H.-J., Zhang, B., Lei, W.-H., Li, Y., & Lasky, P. D. 2015, ApJ, 805, 89
MacFadyen, A. I., & Woosley, S. E. 1999, ApJ, 524, 262
Nakar, E. 2007, PhR, 442, 166
Margutti, R., Berger, E., Fong, W., et al. 2012, ApJ, 756, 63
Metzger, B. D., Giannios, D., Thompson, T. A., Bucciantini, N., & Quataert, E. 2011, MNRAS, 413, 2031
Mészáros, P. 2002, ARA&A, 40, 137
Mundell, C. G., Kopač, D., Arnold, D. M., et al. 2013, Natur, 504, 119
Narayan, R., Paczyński, B., & Piran, T. 1992, ApJL, 395, L83
Nicuesa Guelbenzu, A., Klose, S., Krühler, T., et al. 2012, A&A, 538, L7
Nicuesa Guelbenzu, A., Klose, S., Rossi, A., et al. 2011, A&A, 531, L6
Paczyński, B. 1991, AcA, 41, 257
Popham, R., Woosley, S. E., & Fryer, C. 1999, ApJ, 518, 356
Rosswog, S., & Ramirez-Ruiz, E. 2002, MNRAS, 336, L7
Rosswog, S., Ramirez-Ruiz, E., & Davies, M. B. 2003, MNRAS, 345, 1077
Ruffert, M., & Janka, H.-T. 1998, A&A, 338, 535
Ruffert, M., & Janka, H.-T. 2001, A&A, 380, 544
Sari, R. 1997, ApJL, 489, L37
Sari, R., Piran, T., Halpern, J. P., et al. 1999, ApJL, 519, L17
Soderberg, A. M., Berger, E., Kasliwal, M., et al. 2006, ApJ, 650, 261
Tanvir, N. R., Levan, A. J., Fruchter, A. S., et al. 2013, Natur, 500, 547
Usov, V. V. 1992, Natur, 357, 472
Woosley, S. E., & Bloom, J. S. 2006, ARA&A, 44, 507
Xue, L., Liu, T., Gu, W.-M., & Lu, J.-F. 2013, ApJS, 207, 23
Yuan, F., & Zhang, B. 2012, ApJ, 757, 56
Zalamea, I., & Beloborodov, A. M. 2011, MNRAS, 410, 2302
Zhang, B. 2006, Natur, 444, 1010
Zhang, B., Fan, Y. Z., Dyks, J., et al. 2006, ApJ, 642, 354
Zhang, B., Liang, E., Page, K. L., et al. 2007b, ApJ, 655, 989
Zhang, B., & Mészáros, P. 2004, IJMPA, 19, 2385
Zhang, B., Zhang, B.-B., Liang, E.-W., et al. 2007a, ApJL, 655, L25